Muon反常磁矩的双圈图量级分析

赵树民

河北大学，物理科学与技术学院

2024年BESIII新物理研讨会

2024年8月26日-30日于国科大杭州高等研究院

1、 muon 的反常磁矩

The SM prediction $a_\mu^{\rm SM} = 116591810(43) \times 10^{-11}$

the updated world average $a_\mu^{\rm Exp} = 116592059(22) \times 10^{-11}$

a notable discrepancy a confidence level of 5.1σ

$$\Delta a_\mu \equiv a_\mu^{\rm Exp} - a_\mu^{\rm SM} = (249 \pm 48) \times 10^{-11}.$$

The anomalous magnetic moment receives contributions from all sectors of the SM, and possibly from New Physics (NP): $a_\mu = a_\mu^{\rm QED} + a_\mu^{\rm EW} + a_\mu^{\rm hadronic} + a_\mu^{\rm NP?}$.

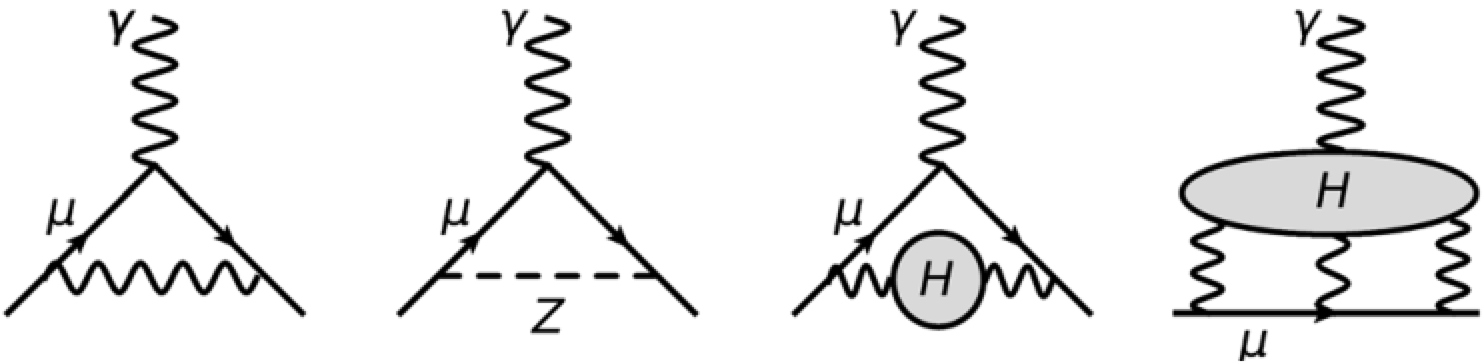

$$a_\mu({\rm SM}) = 116\,591\,810(43) \times 10^{-11} \; (0.37 \;\; {\rm ppm}).$$

2. One loop

arXiv:hep-ph/0609168

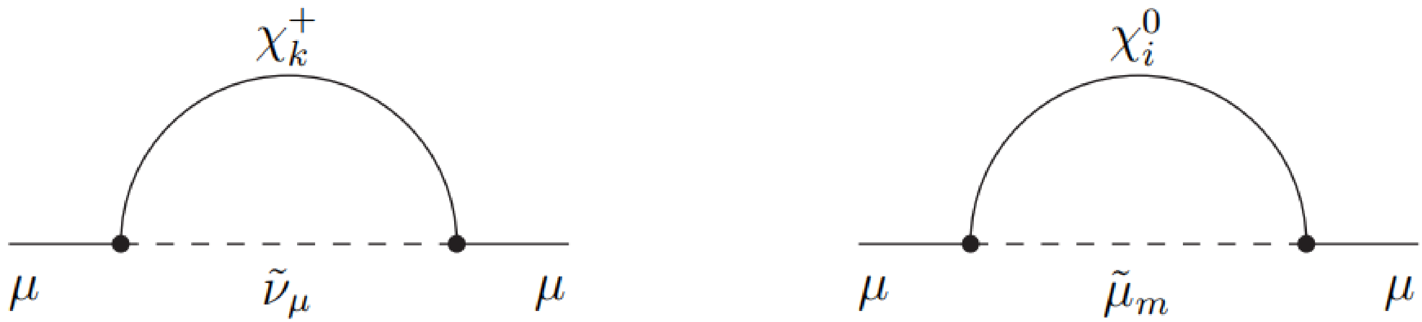

$$a_\mu^{\chi^0} = \frac{m_\mu}{16\pi^2}\sum_{i,m}\left\{-\frac{m_\mu}{12m^2_{\tilde{\mu}_m}}(|n^L_{im}|^2+|n^R_{im}|^2)F_1^N(x_{im})+\frac{m_{\chi_i^0}}{3m^2_{\tilde{\mu}_m}}\mathrm{Re}[n^L_{im}n^R_{im}]F_2^N(x_{im})\right\},$$

$$a_\mu^{\chi^\pm} = \frac{m_\mu}{16\pi^2}\sum_{k}\left\{\frac{m_\mu}{12m^2_{\tilde{\nu}_\mu}}(|c^L_k|^2+|c^R_k|^2)F_1^C(x_k)+\frac{2m_{\chi_k^\pm}}{3m^2_{\tilde{\nu}_\mu}}\mathrm{Re}[c^L_k c^R_k]F_2^C(x_k)\right\},$$

$$n^L_{im} = \frac{1}{\sqrt{2}}(g_1N_{i1}+g_2N_{i2})U^{\tilde{\mu}}_{m1}{}^* - y_\mu N_{i3}U^{\tilde{\mu}}_{m2}{}^*, \qquad c^L_k = -g_2V_{k1},$$

$$n^R_{im} = \sqrt{2}g_1N_{i1}U^{\tilde{\mu}}_{m2} + y_\mu N_{i3}U^{\tilde{\mu}}_{m1}, \qquad c^R_k = y_\mu U_{k2}.$$

it is noteworthy that the terms linear in $m_{\chi^{0,\pm}}$ are not enhanced by a factor $m_{\chi^{0,\pm}}/m_\mu$

these terms involve either an explicit factor of the muon Yukawa coupling y_μ or of the combination $U^{\tilde\mu}_{m1}U^{\tilde\mu}_{m2}/m^2_{\tilde\mu_m}$, which in turn is proportional to $(M^2_\mu)_{12}$ and thus to y_μ. Hence, all terms are of the same basic order $m^2_\mu/M^2_{\rm SUSY}$, and the terms linear in $m_{\chi^{0,\pm}}$ are enhanced merely by a factor $\tan\beta$ from the muon Yukawa coupling.

$$F_2^C(x) = \frac{3}{(1-x)^3}\left[-3+4x-x^2-2\log x\right],$$

$$X = \begin{pmatrix} M_2 & M_W\sqrt{2}\sin\beta \\ M_W\sqrt{2}\cos\beta & \mu \end{pmatrix},$$

$$U^* X V^{-1} = {\rm diag}(m_{\chi_1^\pm}, m_{\chi_2^\pm}).$$

For example, the factors $m_{\chi_k^\pm} c_k^L c_k^R F_2^C(x_k)$ appearing in $a_\mu^{\chi^\pm}$ can be approximated as

$$-g_2 y_\mu \sum_k U_{k2} V_{k1} m_{\chi_k^\pm} \left(\frac{7}{4} - \frac{3}{4} \frac{m^2_{\chi_k^\pm}}{m^2_{\tilde{\nu}_\mu}} \right)$$

$$\approx \frac{3 g_2 y_\mu}{4} \frac{X_{22} (X^\dagger)_{21} X_{11}}{m^2_{\tilde{\nu}_\mu}} \approx \frac{3 g_2 y_\mu}{4} \mathrm{sign}(\mu M_2) X_{12}.$$

$$y_\mu = \frac{m_\mu}{v_1} = \frac{m_\mu g_2}{\sqrt{2} M_W \cos\beta},$$

$$X_{12} = M_W \sqrt{2} \sin\beta$$

$$a_\mu^{\chi^0} = \frac{g_1^2 - g_2^2}{192\pi^2} \frac{m_\mu^2}{M^2_{\mathrm{SUSY}}} \ \mathrm{sign}(\mu M_2) \ \tan\beta \ \left[1 + \mathcal{O}\left(\frac{1}{\tan\beta}, \frac{M_W}{M_{\mathrm{SUSY}}} \right) \right],$$

$$a_\mu^{\chi^\pm} = \frac{g_2^2}{32\pi^2} \ \frac{m_\mu^2}{M^2_{\mathrm{SUSY}}} \ \mathrm{sign}(\mu M_2) \ \tan\beta \ \left[1 + \mathcal{O}\left(\frac{1}{\tan\beta}, \frac{M_W}{M_{\mathrm{SUSY}}} \right) \right],$$

2、双圈图量级分析

以MSSM为例对双圈图量级进行分析

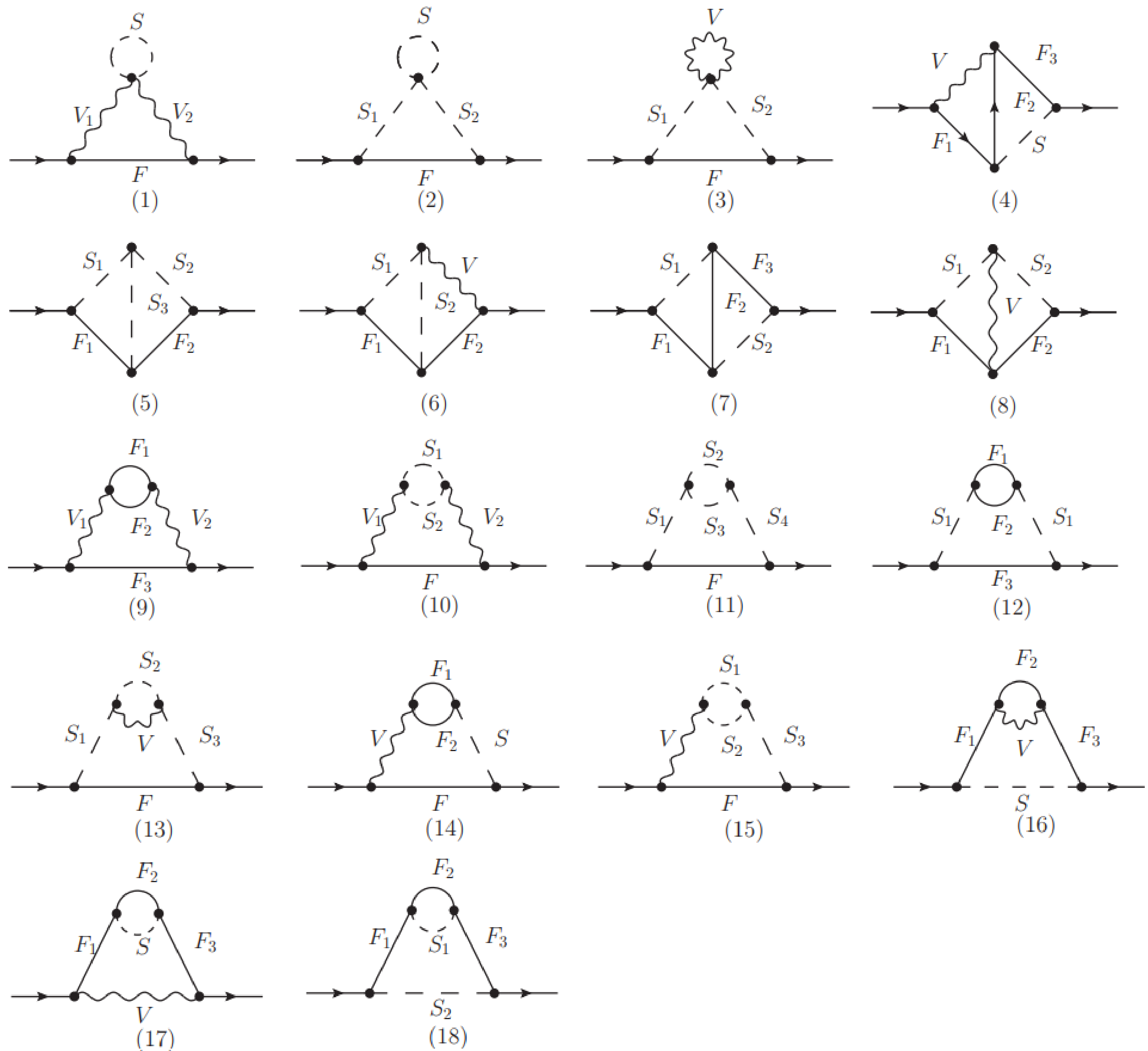

We take two examples to explain the conversion between the two loop self-energy diagrams in mass eigenstate and the corresponding diagrams in electroweak eigenstate for MIA.

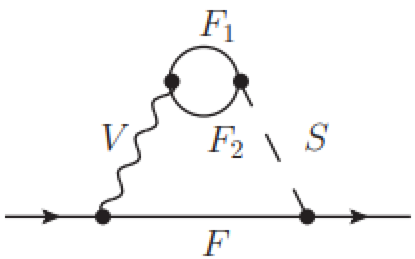

(14)

we take $V=\gamma,\ F=\mu,\ S=h^0,\ F_1=F_2=\chi^{\pm},$

The factor is $\frac{x_l}{x_M^{1/2}x_V^{1/2}}$

which has the suppression factor $\frac{m_l}{m_V}=\frac{x_l^{1/2}}{x_V^{1/2}}$ in the vertex.

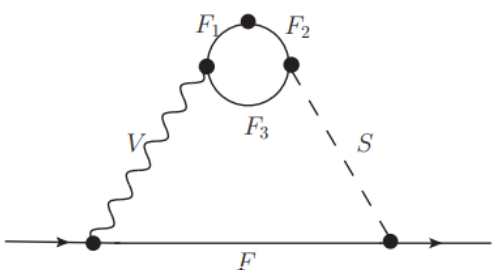

$V=\gamma,\ F=\mu,\ S=h_d^0,$

$F_1=\tilde{W}^{\pm}, F_2=\tilde{H}^{\pm}, F_3=\tilde{W}^{\pm}.$

The contribution to muon MDM from this diagram has the factor $\frac{m_\mu^2}{M_{NP}^2}\frac{\mu M_2}{M_{NP}^2}\tan\beta$, and it can be simplified as $\frac{m_\mu^2}{M_{NP}^2}\tan\beta$ with the supposition $\mu\sim M_2\sim M_{NP}$.

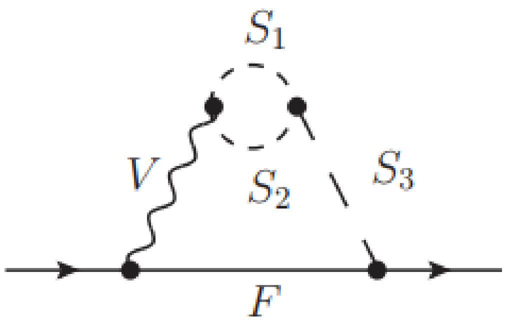

$V=\gamma,\ F=\mu,\ S_1=\tilde{t}\ ,\ S_2=\tilde{t}\ ,\ S_3=h^0.$

In the end, these type diagrams

give muon MDM corrections with two factors: $\frac{x_l\lambda_{HSS}}{x_V^{1/2}x_M^{1/2}M}$

and $\frac{x_l\lambda_{HSS}}{x_V^{1/2}x_H^{1/2}m_H}$. In rough estimation, $\frac{\lambda_{HSS}}{m_H}\lesssim 1$.

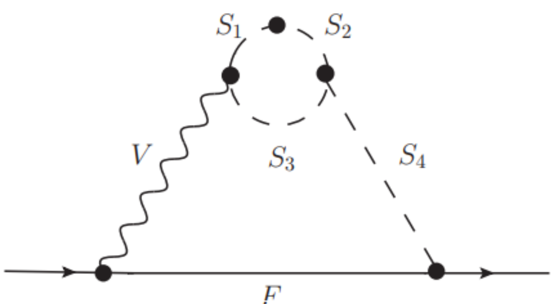

$V=\gamma,\ F=\mu,\ S_1=\tilde{t}_R,\ S_2=\tilde{t}_L,\ S_3=\tilde{t}_R,\ S_4=h_d^0.$

this diagram has the typical parameter

$$\frac{m_\mu^2}{M_{NP}^2}\tan\beta\frac{\mu m_t}{m_W^2}\frac{m_t(A_t-\mu^*\cot\beta)}{M_{NP}^2}\sim\frac{m_\mu^2}{M_{NP}^2}\tan\beta\frac{\mu m_t}{m_W^2}\frac{m_t A_t}{M_{NP}^2}$$

$$\sim\frac{m_\mu^2}{M_{NP}^2}\tan\beta\frac{m_t^2}{m_W^2}\sim 4.6\times\frac{m_\mu^2}{M_{NP}^2}\tan\beta.$$

For this type diagram, when the particles in the scalar sub-loop are Higgs, the corresponding factors are shown as follows $\frac{m_\mu^2}{M_{NP}^2}\tan\beta\frac{B_\mu}{M_{NP}^2}\sim\frac{m_\mu^2}{M_{NP}^2}\tan\beta.$

Here B_μ is at the order of M_{NP}^2. From the above analysis, one can find $\frac{m_\mu^2}{M_{NP}^2}\tan\beta$ is the typical factor.

For a concise display of results, we collect the diagrams possess the same factor. To simplify the discussion, we adopt the supposition $M_Z \sim M_W \sim M_V$.

1. The diagrams have the factor $\frac{m_\mu^2}{M_{NP}^2}$ are

$$\text{Fig.1(1)}\Big\{\gamma;\ S;\ (\gamma,\ Z);\ \mu\Big\},\ \text{Fig.1(9)}\Big\{\chi^\pm;\ \chi^\pm;\ \mu;\ \gamma;\ (\gamma,\ Z)\Big\},$$
$$\text{Fig.1(10)}\Big\{S;\ S;\ \gamma;\ (\gamma,\ Z);\ \mu\Big\}.$$

with S denoting the charged scalar particles $(\tilde{L},\ \tilde{U},\ \tilde{D},\ H^\pm)$. The factor $\frac{m_\mu^2}{M^2}$ does not have the improvement term large $\tan\beta$, so these diagrams can be neglected safely.

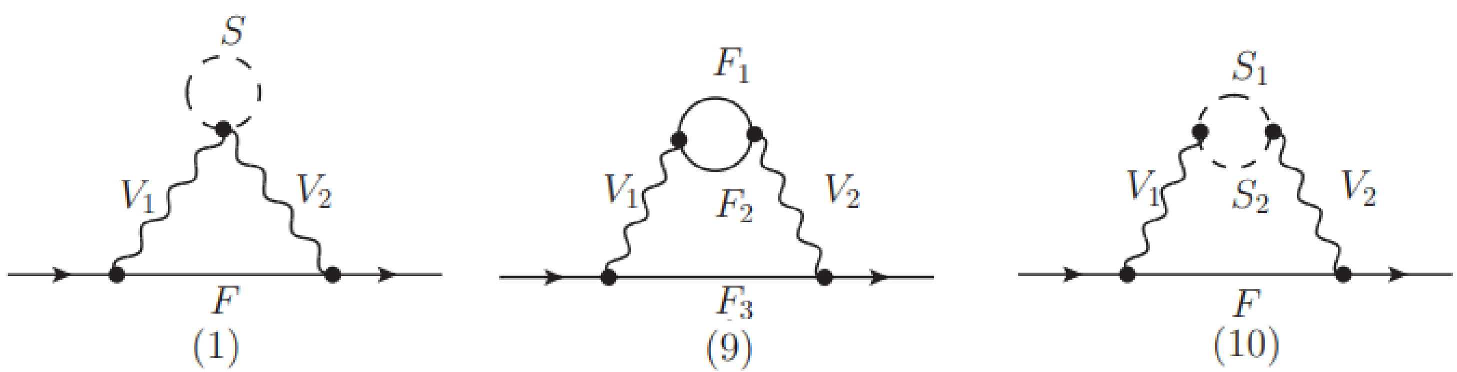

2. The factor $\frac{m_\mu^2}{M_V^2}$ is large, which is bigger than the factor $\frac{m_\mu^2}{M^2}\tan\beta$ with $M \sim 1000$GeV. Supposing $M_V \sim 90$GeV and $\tan\beta \sim 50$, the ratio of the first factor to the second factor is

$$\frac{\frac{m_\mu^2}{M_V^2}}{\frac{m_\mu^2}{M^2}\tan\beta} = \frac{M^2}{M_V^2\tan\beta} = \frac{1000^2}{90^2\times 50} \sim 2.47.$$

$$\text{Fig.1(1)}\Big\{Z;\ S;\ Z;\ \mu\Big\}, \qquad \text{Fig.1(1)}\Big\{W;\ S;\ W;\ \nu\Big\},$$
$$\text{Fig.1(9)}\Big\{\chi^0;\ \chi^\pm;\ \nu;\ W;\ W\Big\}, \quad \text{Fig.1(9)}\Big\{\chi^\pm;\ \chi^\pm;\ \mu;\ Z;\ Z\Big\},$$
$$\text{Fig.1(10)}\Big\{S;\ S;\ Z;\ Z;\ \mu\Big\}, \qquad \text{Fig.1(10)}\Big\{S1;\ S2;\ W;\ W;\ \nu\Big\},$$

with $S = \tilde{L},\ H^\pm,\ \tilde{U},\ \tilde{D},\ H^0(A^0),\ \tilde{\nu}$
and $(S1,\ S2) = (\tilde{\nu},\ \tilde{L});\ (\tilde{U},\ \tilde{D});\ (H^0,\ H^\pm)$.

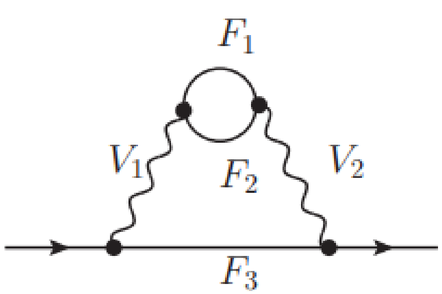

(9)

In on-shell scheme, the contribution from $\text{Fig.1(9)}\Big\{\chi^0;\ \chi^0;\ \mu;\ Z;\ Z\Big\}$ does not have large factor $\frac{m_\mu^2}{M_V^2}$, and it is classified as negligible

3. There are many two loop diagrams including several types that have the typical factor $\frac{m_\mu^2}{M^2} \tan\beta$.

These two loop self-energy diagrams account for more than half of all two loop diagrams.

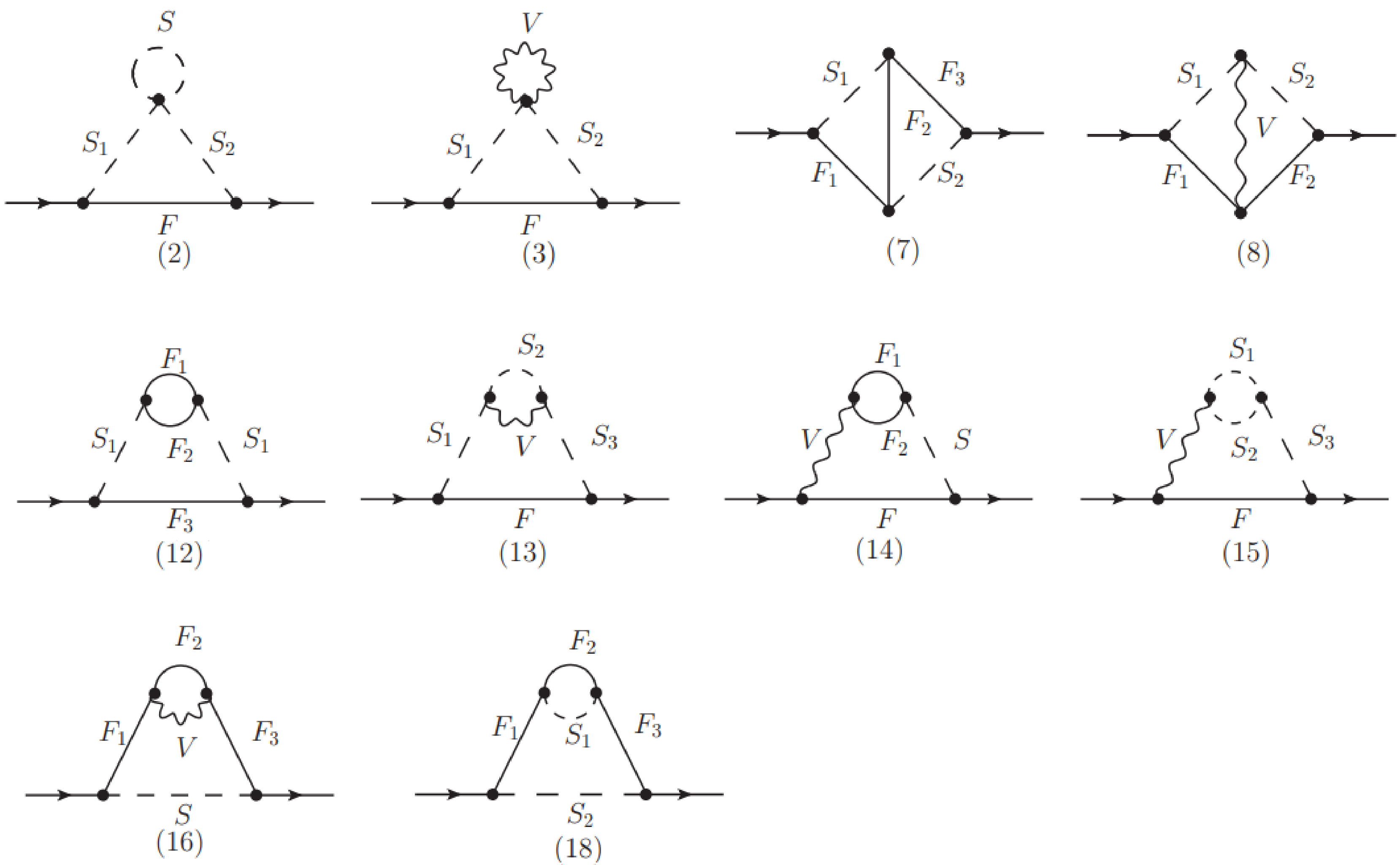

Fig.1(2)$\left\{\tilde{L};\ S;\ \tilde{L};\ \chi^0\right\}$, Fig.1(2)$\left\{\tilde{\nu};\ S;\ \tilde{\nu};\ \chi^\pm\right\}$, with $S=\tilde{\nu},\ \tilde{L},\ H^0,\ H^\pm$,

Fig.1(3)$\left\{\tilde{L};\ \tilde{L};\ (\gamma,\ Z,\ W);\ \chi^0\right\}$, Fig.1(3)$\left\{\tilde{\nu};\ \tilde{\nu};\ (Z,\ W);\ \chi^\pm\right\}$,

Fig.1(7)$\left\{\chi^0;\ \mu;\ \chi^0;\ \tilde{L};\ \tilde{L}\right\}$, Fig.1(7)$\left\{\chi^\pm;\ \mu;\ \chi^\pm;\ \tilde{\nu};\ \tilde{\nu}\right\}$,

Fig.1(7)$\left\{\chi^0;\ \nu;\ \chi^\pm;\ \tilde{L};\ \tilde{\nu}\right\}$, Fig.1(8)$\left\{\chi^0;\ \chi^\pm;\ \tilde{L};\ \tilde{\nu};\ W\right\}$,

Fig.1(8)$\left\{\chi^\pm;\ \chi^\pm;\ \tilde{\nu};\ \tilde{\nu};\ Z\right\}$, Fig.1(8)$\left\{\chi^0;\ \chi^0;\ \tilde{L};\ \tilde{L};\ Z\right\}$,

Fig.1(12)$\left\{\mu;\ \chi^\pm;\ \chi^\pm;\ \tilde{\nu};\ \tilde{\nu}\right\}$, Fig.1(12)$\left\{\mu;\ \chi^0;\ \chi^0;\ \tilde{L};\ \tilde{L}\right\}$,

Fig.1(12)$\left\{\nu;\ \chi^\pm;\ \chi^0;\ \tilde{L};\ \tilde{L}\right\}$, Fig.1(12)$\left\{\nu;\ \chi^0;\ \chi^\pm;\ \tilde{\nu};\ \tilde{\nu}\right\}$,

Fig.1(13)$\left\{\tilde{L};\ \tilde{L};\ \tilde{L};\ (\gamma,\ Z);\ \chi^0\right\}$, Fig.1(13)$\left\{\tilde{\nu};\ \tilde{\nu};\ \tilde{\nu};\ Z;\ \chi^\pm\right\}$,

Fig.1(13)$\left\{\tilde{\nu};\ \tilde{L};\ \tilde{\nu};\ W;\ \chi^\pm\right\}$, Fig.1(13)$\left\{\tilde{L};\ \tilde{\nu};\ \tilde{L};\ W;\ \chi^0\right\}$,

Fig.1(14)$\left\{\chi^\pm;\ \chi^\pm;\ \mu;\ Z;\ H^0\right\}$, Fig.1(14)$\left\{\chi^\pm;\ \chi^0;\ \nu;\ W;\ H^\pm\right\}$,

Fig.1(15)$\left\{\tilde{t};\ \tilde{b};\ H^0;\ W;\ \nu\right\}$, Fig.1(15)$\left\{\tilde{t};\ \tilde{t};\ H^0;\ Z;\ \mu\right\}$,

Fig.1(15)$\left\{\tilde{L};\ \tilde{L};\ H^0;\ (\gamma,\ Z);\ \mu\right\}$, Fig.1(15)$\left\{\tilde{D};\ \tilde{D};\ H^0;\ (\gamma,\ Z);\ \mu\right\}$,

Fig.1(15)$\left\{\tilde{\nu};\ \tilde{\nu};\ H^0;\ Z;\ \mu\right\}$, Fig.1(15)$\left\{\tilde{L};\ \tilde{\nu};\ H^\pm;\ W;\ \nu\right\}$,

Fig.1(15)$\left\{H^\pm;\ H^\pm;\ H^0;\ (\gamma,\ Z);\ \mu\right\}$, Fig.1(15)$\left\{H^0;\ A^0;\ A^0;\ Z;\ \mu\right\}$,

Fig.1(15)$\left\{H^\pm;\ (A^0,\ H^0);\ H^\pm;\ W;\ \nu\right\}$.

$$\text{Fig.1(16)}\Big\{\chi^0;\ \chi^\pm;\ \chi^0;\ W;\ \tilde{L}\Big\}, \qquad \text{Fig.1(16)}\Big\{\chi^0;\ \chi^0;\ \chi^0;\ Z;\ \tilde{L}\Big\},$$

$$\text{Fig.1(16)}\Big\{\chi^\pm;\ \chi^\pm;\ \chi^\pm;\ (\gamma,\ Z);\tilde{\nu}\Big\}, \qquad \text{Fig.1(16)}\Big\{\chi^\pm;\ \chi^0;\ \chi^\pm;\ W;\ \tilde{\nu}\Big\},$$

$$\text{Fig.1(18)}\Big\{\chi^\pm;\ \chi^\pm;\ \chi^\pm;\ H^0;\ \tilde{\nu}\Big\}, \qquad \text{Fig.1(18)}\Big\{\chi^\pm;\ \chi^0;\ \chi^\pm;\ H^\pm;\ \tilde{\nu}\Big\},$$

$$\text{Fig.1(18)}\Big\{\chi^0;\ \chi^0;\ \chi^0;\ H^0;\ \tilde{L}\Big\}, \qquad \text{Fig.1(18)}\Big\{\chi^0;\ \chi^\pm;\ \chi^0;\ H^\pm;\ \tilde{L}\Big\},$$

$$\text{Fig.1(18)}\Big\{\chi^0;\ F;\ \chi^0;\ \tilde{S};\ \tilde{L}\Big\}, \qquad \text{with } (F,\ \tilde{S}) = (\nu,\ \tilde{\nu}),\ (l,\ \tilde{L}),$$

$$\text{Fig.1(18)}\Big\{\chi^\pm;\ F;\ \chi^\pm;\ \tilde{S};\ \tilde{\nu}\Big\}, \qquad \text{with } (F,\ \tilde{S}) = (\nu,\ \tilde{L}),\ (l,\ \tilde{\nu}).$$

4. The following diagrams in Eq.(11) have the very large factor $\frac{m_\mu^2}{M_V^2}\tan\beta$. So these diagrams are most important to study muon MDM.

$$\text{Fig.1(4)}\{\nu;\ \chi^0;\ \chi^\pm;\ W;\ \tilde{\nu}\},\qquad \text{Fig.1(4)}\{\nu;\ \chi^\pm;\ \chi^0;\ W;\ \tilde{L}\},$$

$$\text{Fig.1(4)}\{\mu;\ \chi^0;\ \chi^0;\ Z;\ \tilde{L}\},\qquad \text{Fig.1(4)}\{\mu;\ \chi^\pm;\ \chi^\pm;\ Z;\ \tilde{\nu}\},$$

$$\text{Fig.1(6)}\{\chi^\pm;\ \mu;\ \tilde{\nu};\ \tilde{\nu};\ Z\},\qquad \text{Fig.1(6)}\{\chi^0;\ \mu;\ \tilde{L};\ \tilde{L};\ Z\},$$

$$\text{Fig.1(6)}\{\chi^0;\ \nu;\ \tilde{L};\ \tilde{\nu};\ W\},\qquad \text{Fig.1(6)}\{\chi^\pm;\ \nu;\ \tilde{\nu};\ \tilde{L};\ W\},$$

$$\text{Fig.1(17)}\{\nu;\ \chi^\pm;\ \nu;\ \tilde{L};\ W\},\qquad \text{Fig.1(17)}\{\nu;\ \chi^0;\ \nu;\ \tilde{\nu};\ W\},$$

$$\text{Fig.1(17)}\{\mu;\ \chi^0;\ \mu;\ \tilde{L};\ Z\},\qquad \text{Fig.1(17)}\{\mu;\ \chi^\pm;\ \mu;\ \tilde{\nu};\ Z\}.$$

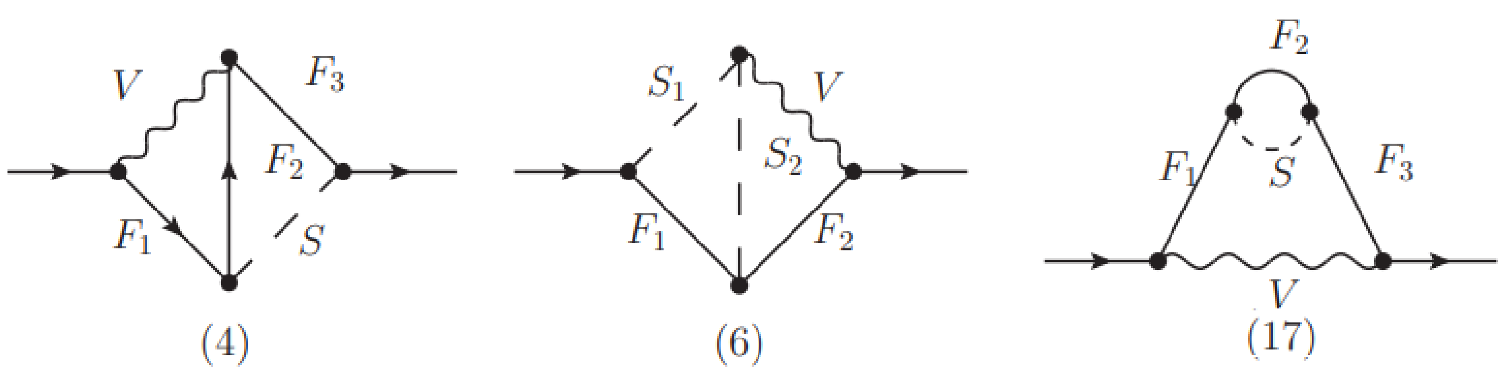

5. This type diagrams have the vertex $S-H-S$ possessing mass dimension, which is supposed as λ_{HSS}. Their contributions have the factor $\frac{m_\mu^2}{M_{NP}^2}\tan\beta\times\frac{\lambda_{HSS}}{M_{NP}}$, which is not larger than $\frac{m_\mu^2}{M_{NP}^2}\tan\beta$.

Fig.1(5)$\Big\{\chi^\pm;\ \chi^\pm;\ \tilde{\nu};\ \tilde{\nu};\ H^0\Big\}$, Fig.1(5)$\Big\{\chi^0;\ \chi^0;\ \tilde{L};\ \tilde{L};\ H^0\Big\}$, Fig.1(5)$\Big\{\chi^0;\ \chi^\pm;\ \tilde{L};\ \tilde{\nu};\ H^\pm\Big\}$.

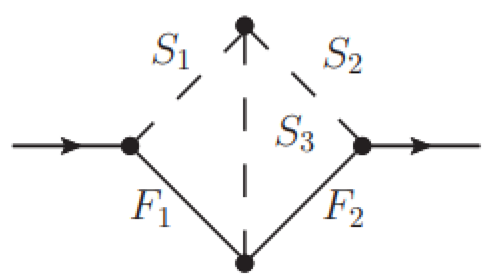

(5)

6. Similar as the above condition, this type diagram has two vertexes $H-S-S$ and the couplings λ_{HSS}^2.

From analysis, their typical factor is $\frac{m_\mu^2}{M_{NP}^2}\tan\beta \times \frac{\lambda_{HSS}^2}{M_{NP}^2} \leq \frac{m_\mu^2}{M_{NP}^2}\tan\beta$. Because λ_{HSS} is not larger than M_{NP} in general.

Fig.1(11)$\{\tilde{\nu};\ H^0;\ \tilde{\nu};\ \tilde{\nu};\ \chi^\pm\}$, Fig.1(11)$\{\tilde{\nu};\ H^\pm;\ \tilde{L};\ \tilde{\nu};\ \chi^\pm\}$,

Fig.1(11)$\{\tilde{L};\ H^0;\ \tilde{L};\ \tilde{L};\ \chi^0\}$, Fig.1(11)$\{\tilde{L};\ H^\pm;\ \tilde{\nu};\ \tilde{L};\ \chi^0\}$.

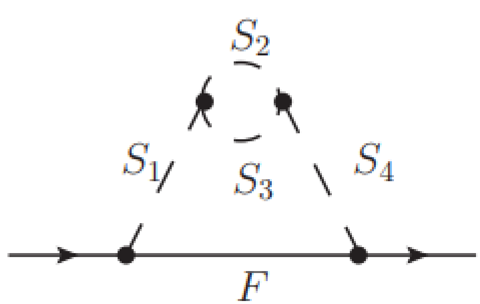

(11)

7. This type diagram Fig.1(18)$\Big\{F1; F2; F3; S1; S2\Big\}$ has been researched by the authors.

In our supposition, this type diagram also has the typical factor $\frac{m_\mu^2}{M_{NP}^2}\tan\beta$. If the internal sfermions are very heavy, they can produce non-decoupling and logarithmically enhanced contributions to muon MDM. Supposing that the mass of heavy squark is M_{SH} and $M_{SH} \gg M$, the logarithmically enhanced factor $\log\frac{M_{SH}^2}{M_{NP}^2}$ appears leading to the factor $\frac{m_\mu^2}{M_{NP}^2}\tan\beta\log\frac{M_{SH}^2}{M_{NP}^2}$.

$$\text{Fig.1(18)}\Big\{\chi^0;\ F;\ \chi^0;\ \tilde{S};\ \tilde{L}\Big\} \text{ with } (F,\ \tilde{S}) = (u_i,\ \tilde{U}),\ (d_i,\ \tilde{D}),$$

$$\text{Fig.1(18)}\Big\{\chi^\pm;\ F;\ \chi^\pm;\ \tilde{S};\ \tilde{\nu}\Big\} \text{ with } (F,\ \tilde{S}) = (u_i,\ \tilde{D}),\ (d_i,\ \tilde{U}).$$

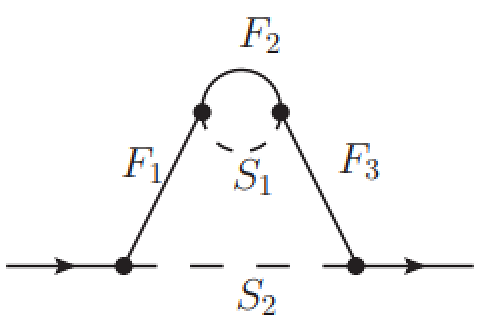

(18)

H.G. Fargnoli, C. Gnendiger, S. Paßehr, D. Stöckinger, H. Stöckinger-Kim, Phys. Lett. B **726**, 717 (2013)

8. The diagrams in Eq.(15) all have the lepton-Higgs-lepton vertexes, which lead to additional suppression factor $\frac{m_\mu}{Vew}\tan\beta \lesssim 0.02$. Their total factors are shown as $\left(\frac{m_\mu^2}{M_H^2}\tan\beta,\ \frac{m_\mu^2}{M_{NP}^2}\tan\beta\right) \times \frac{m_\mu}{Vew}\tan\beta$, which can be neglected safely.

$$\text{Fig.1(7)}\Big\{\mu;\ \chi^\pm;\ \chi^\pm;\ H^0;\ \tilde{\nu}\Big\},\ \ \text{Fig.1(7)}\Big\{\mu;\ \chi^0;\ \chi^0;\ H^0;\ \tilde{L}\Big\},$$
$$\text{Fig.1(7)}\Big\{\nu;\ \chi^0;\ \chi^\pm;\ H^\pm;\ \tilde{\nu}\Big\},\ \ \text{Fig.1(7)}\Big\{\nu;\ \chi^\pm;\ \chi^0;\ H^\pm;\ \tilde{L}\Big\}.$$

This type can be neglected!

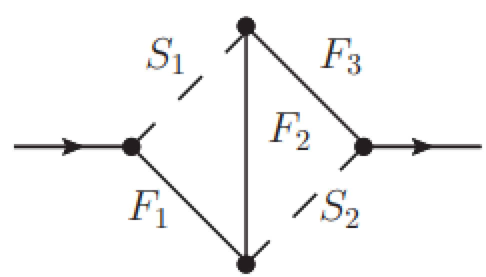

(7)

9. The factor $\frac{m_\mu^2}{M_{NP}^2}\tan\beta\log x_\mu$ is larger than the factor $\frac{m_\mu^2}{M_{NP}^2}\tan\beta$, because $\log\frac{m_\mu}{M_{NP}} \sim -9$ with $M_{NP} = 1000\text{GeV}$. This factor is negative, and is enhanced by one order of magnitude by the large logarithmic function.

This condition has been discussed by the authors for the two loop diagrams in which the internal photon couples to at least one muon. If the internal photon is deleted, these two loop diagrams turn to the one loop SUSY diagrams of $\mu \to \mu$, where the internal particles are slepton-neutralino and sneutrino-chargino.

$$\text{Fig.1(4)}\left\{\mu;\ \chi^\pm;\ \chi^\pm;\ \gamma;\ \tilde{\nu}\right\}, \qquad \text{Fig.1(6)}\left\{\chi^0;\ \mu;\ \tilde{L};\ \tilde{L};\ \gamma\right\},$$

$$\text{Fig.1(17)}\left\{\mu;\ \chi^\pm;\ \mu;\ \tilde{\nu};\ \gamma\right\}, \qquad \text{Fig.1(17)}\left\{\mu;\ \chi^0;\ \mu;\ \tilde{L};\ \gamma\right\}.$$

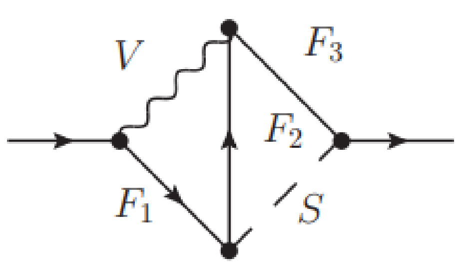

(4)

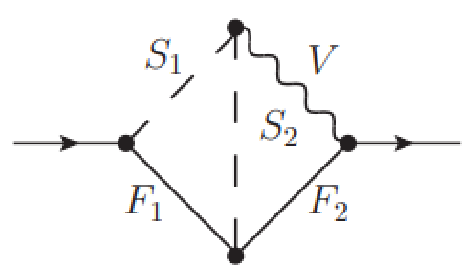

(6)

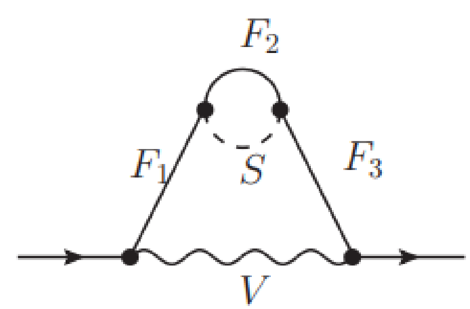

(17)

Summary

质量本征态下的量级

1 The large factors $\frac{x_l^{1/2}}{x_M^{1/2}}$ and $\frac{x_l}{x_V}$.

2 Because $\frac{\lambda_{HSS}}{M}$, $\frac{\lambda_{HSS}^2}{M^2}$, $\frac{\lambda_{HSS}^2}{m_H^2}$ and $\frac{m_F}{M}$ are not more than 1,

$(\frac{x_l^{1/2}\lambda_{HSS}}{x_M^{1/2}M}, \frac{x_l^{1/2}\lambda_{HSS}^2}{x_M^{1/2}M^2}, \frac{x_l^{1/2}\lambda_{HSS}^2}{x_M^{1/2}m_H^2}, \frac{x_l^{1/2}}{x_M^{1/2}}\frac{m_F}{M})$ should not be bigger than the factor $\frac{x_l^{1/2}}{x_M^{1/2}}$.

3 The middle factors $\frac{x_l}{x_M^{1/2}x_V^{1/2}}$ $\frac{x_l\lambda_{HSS}}{x_V^{1/2}x_M^{1/2}M}$ and $\frac{x_l\lambda_{HSS}}{x_V^{1/2}x_H^{1/2}m_H}$.

4 The small factors $\frac{x_l}{x_M}$ and $\frac{x_l^{3/2}}{x_H x_V^{1/2}}$.

5 The non-decoupling factor $\frac{x_l^{1/2}}{x_M^{1/2}}\frac{m_F}{M}\log x_{SH}$ is special.

质量插入近似法下的量级

1 From these factors, one can find that $\frac{m_\mu^2}{M_{NP}^2}, \frac{m_\mu^2}{M_H^2}\tan\beta\frac{m_\mu}{Vew}\tan\beta, \frac{m_\mu^2}{M_{NP}^2}\tan\beta\frac{m_\mu}{Vew}\tan\beta$ are small, and can be ignored safely.

2 The considerable factors are $\frac{m_\mu^2}{M_{NP}^2}\tan\beta$, $\frac{m_\mu^2}{M_V^2}$, $\frac{m_\mu^2}{M_{NP}^2}\tan\beta\frac{\lambda_{HSS}}{M_{NP}}$, $\frac{m_\mu^2}{M_{NP}^2}\tan\beta\frac{\lambda_{HSS}^2}{M_{NP}^2}$. Most two loop diagrams possess the typical factor $\frac{m_\mu^2}{M^2}\tan\beta$.

3 The rest are big ones including $\frac{m_\mu^2}{M_V^2}\tan\beta$ and $\frac{m_\mu^2}{M_{NP}^2}\tan\beta\log\frac{m_\mu}{M_{NP}}$. The large logarithm $\log\frac{m_\mu}{M_{NP}}$ gives negative corrections.

4 if squarks are very heavy, the corrections from Fig.1(18) type diagram are non-decoupling and logarithmically enhanced with $\frac{m_\mu^2}{M_{NP}^2}\tan\beta\log\frac{M_{SH}^2}{M_{NP}^2}$.


谢谢